



## Assignment of amide proton signals by combined evaluation of HN, NN and HNCA MAS-NMR correlation spectra

Barth-Jan van Rossum<sup>a</sup>, Federica Castellani<sup>a</sup>, Jutta Pauli<sup>a,\*</sup>, Kristina Rehbein<sup>a</sup>, J. Hollander<sup>b</sup>, Huub J.M. de Groot<sup>b</sup> & Hartmut Oschkinat<sup>a,\*\*</sup>

<sup>a</sup>Forschungsinstitut für Molekulare Pharmakologie (FMP), Robert-Rössle Str. 10, D-13125, Berlin, Germany

<sup>b</sup>Gorlaeus Laboratories, University of Leiden, P.O. Box 9502, 2300 RA, Leiden, The Netherlands

Received 16 September 2002; Accepted 20 December 2002

**Key words:** assignment, dipolar correlation spectroscopy, magic-angle-spinning, SH3 domain, solid-state MAS NMR

### Abstract

In this paper, we present a strategy for the <sup>1</sup>H<sup>N</sup> resonance assignment in solid-state magic-angle spinning (MAS) NMR, using the α-spectrin SH3 domain as an example. A novel 3D triple resonance experiment is presented that yields intraresidue H<sup>N</sup>-N-C<sup>α</sup> correlations, which was essential for the proton assignment. For the observable residues, 52 out of the 54 amide proton resonances were assigned from 2D (<sup>1</sup>H-<sup>15</sup>N) and 3D (<sup>1</sup>H-<sup>15</sup>N-<sup>13</sup>C) heteronuclear correlation spectra. It is demonstrated that proton-driven spin diffusion (PDS) experiments recorded with long mixing times (4 s) are helpful for confirming the assignment of the protein backbone <sup>15</sup>N resonances and as an aid in the amide proton assignment.

### Introduction

MAS solid-state NMR is rapidly developing into a versatile tool for the structural investigation of biological systems that cannot be studied with solution NMR and which do not easily form 3D crystals, such as aggregates of soluble proteins or peptides and membrane proteins (Castellani et al., 2002; Griffin, 1998). Prior to the detection of structural restraints that form the input of structure calculations, assignment of the protein resonances is mandatory. In the past few years, several groups reported on solid-state NMR assignment strategies for multiply-enriched, small proteins (Straus et al., 1998; Hong, 1999; Pauli et al., 2000, 2001; McDermott et al., 2000; van Rossum et al., 2001). The <sup>15</sup>N chemical shifts play there a key-role, since sequence-specific assignment procedures often rely on heteronuclear correlations between the amide <sup>15</sup>N and the C<sup>α</sup> of the same amino acid or the CO of

the previous one in the sequence. Using triple resonance techniques, almost complete assignments of the <sup>13</sup>C and <sup>15</sup>N resonances of the α-spectrin SH3 domain were achieved (Pauli et al., 2001). The resonances of non-exchangeable protons were assigned by 3D <sup>1</sup>H-<sup>13</sup>C-<sup>13</sup>C correlation spectroscopy (van Rossum et al., 2001). In this paper, we focus on strategies for the assignment of amide proton signals. This is the third paper in a series and, with the assignment of the amide protons, it completes the solid-state MAS NMR assignment of the α-spectrin SH3 domain (van Rossum et al., 2001; Pauli et al., 2001), that is used as an example.

NH groups are important structural monitors, since they are often involved in the formation of hydrogen-bonds that stabilise the folding of a protein. In addition, the NH chemical shifts are sensitive to the protein backbone conformations, therefore providing secondary structure information. In static NMR experiments on oriented membranes, the NH chemical shifts and dipolar interaction vectors form the corner stone of the PISEMA experiment (Wu et al., 1994). In MAS NMR, amide <sup>1</sup>H and <sup>15</sup>N nuclei may be used

\*Present address: BAM, Richard-Willstätter-Str. 11, D-12489, Berlin, Germany.

\*\*To whom correspondence should be addressed. E-mail: Oschkinat@fmp-berlin.de

for the detection of N-H...X bond lengths, for the measurement of torsion angles or of HH distance restraints (Hong et al., 1997; Schnell et al., 1998; Reif et al., 2000; Hohwy et al., 2000; Brown et al., 2001; Zhao et al., 2001; Song and McDermott, 2001). In particular, for the detection of long-range H-H correlations, the amide protons are potentially useful due to their high  $\gamma$ , once samples that are perdeuterated at the non-exchangeable sites are provided. Perdeuteration removes all strong  $^1\text{H}$ - $^1\text{H}$  dipolar couplings and leads to relatively well-resolved proton spectra, while applying mild  $^1\text{H}$ -homonuclear decoupling. This makes a semi-quantitative analysis of transfer events and cross-peak intensities feasible, as demonstrated in a recent communication (Reif et al., submitted).

## Materials and methods

Samples of the  $\alpha$ -spectrin SH3 domain were prepared as described previously (Pauli et al., 2000). For the solid-state CP/MAS NMR correlation experiments, preparations containing typically  $\sim 1.4$   $\mu\text{mol}$  (10 mg) of ( $U$ - $^{15}\text{N}$ ) or ( $U$ - $^{13}\text{C}$ ,  $^{15}\text{N}$ )  $\alpha$ -spectrin SH3 domain were used. The samples were confined to the centre of the rotor by use of spacers to optimise RF homogeneity.

All solid-state spectra were recorded with a MAS frequency  $\omega_R/2\pi = 8.0$  kHz. The 2D  $^1\text{H}$ - $^{15}\text{N}$  and  $^{15}\text{N}$ - $^{15}\text{N}$  dipolar correlation experiments were performed at 298 K at a field of 17.6 T using a wide-bore DMX-750 spectrometer (Bruker, Karlsruhe, Germany). The 3D  $^1\text{H}$ - $^{15}\text{N}$ - $^{13}\text{C}$  dataset was recorded at 280 K, with a DMX-400 spectrometer operating at a field of 9.4 T (Bruker, Karlsruhe, Germany). Both spectrometers were equipped with 4 mm triple-resonance CP/MAS probes (Bruker, Karlsruhe, Germany). The heteronuclear correlation experiment was obtained with the pulse program depicted in Figure 1A, which employs phase-modulated Lee-Goldburg (PMLG) irradiation during proton evolution to suppress strong  $^1\text{H}$ -homonuclear dipolar interactions (Vinogradov et al., 1999). For the  $^{15}\text{N}$ -homonuclear correlation experiment, a standard PDS sequence was used, with a mixing time of 4.0 s (Szeverenyi et al., 1982). The 3D  $^1\text{H}$ - $^{15}\text{N}$ - $^{13}\text{C}$  experiment is shown in Figure 1B and applies specific-CP (Baldus et al., 1998) to transfer magnetisation selectively between the amide  $^{15}\text{N}$  and the  $^{13}\text{C}^\alpha$  of the same residue.

For PMLG decoupling a shaped-pulse was used that mimics each frequency offset with a phase trajec-

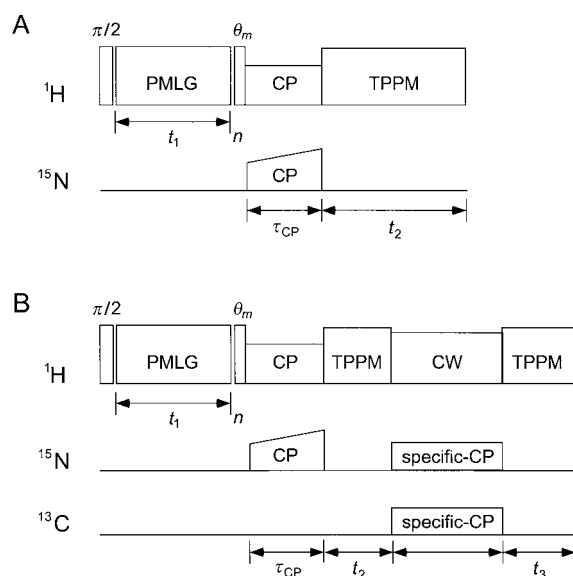


Figure 1. Pulse programs used for the 2D  $^1\text{H}$ - $^{15}\text{N}$  (A) and 3D  $^1\text{H}$ - $^{15}\text{N}$ - $^{13}\text{C}$  (B) dipolar correlation experiments. The  $^1\text{H}$ -homonuclear dipolar interactions were suppressed with PMLG-decoupling (Vinogradov et al., 1999). Heteronuclear decoupling ( $^1\text{H}$ - $^{13}\text{C}$  or  $^1\text{H}$ - $^{15}\text{N}$ ) was achieved with TPPM during evolution and acquisition (Bennett et al., 1995), while continuous wave (CW) decoupling was applied during the specific-CP (Baldus et al., 1998).

tory that contains three phase steps (PMLG-3) (Vinogradov et al., 1999). The shaped pulse contains 2048 complete PMLG cycles and has a total duration  $\tau_{\text{tot}}$ . Prior to the experiments, the efficiency of the PMLG decoupling was optimised using the natural abundance  $^{13}\text{C}$  signals of adamantane. This was done by observing the  $J_{\text{CH}}$ -couplings in 1D  $^{13}\text{C}$  spectra collected with PMLG irradiation during data acquisition, and by fine-tuning the pulse length  $\tau_{\text{tot}}$  to yield optimally resolved doublet and triplet line shapes for the CH and  $\text{CH}_2$  moieties, respectively. The proton evolution in  $t_1$  was sampled at intervals  $\tau_{\text{inc}}$  corresponding to two complete PMLG cycles (typically 40  $\mu\text{s}$ ). The increment  $\tau_{\text{inc}}$  was first calculated according to  $\tau_{\text{tot}}/1024$ , rounded off to the nearest integral multiple of 100 ns. Subsequently,  $\tau_{\text{tot}}$  was recalculated as  $(\tau_{\text{inc}} \cdot 1024)$ . This was done to ensure synchronisation of  $n \cdot \tau_{\text{inc}}$  with the shaped pulse for large  $n$ . For similar reasons, the starting increment for the indirect detection can not be chosen arbitrarily, but should be set to 0  $\mu\text{s}$  or to a small multiple of  $\tau_{\text{inc}}/2$ . The PMLG decoupling was optimised for the SH3 preparations by adjusting the  $^1\text{H}$  RF strength to yield similar  $^1\text{H}$  pulse lengths as found for the adamantane sample. For all SH3 samples

that we have studied, this results in RF powers that are about 10% higher than for adamantane.

The protons were decoupled by use of the two-pulse phase-modulation (TPPM) decoupling scheme during all acquisition periods and during the indirect  $^{15}\text{N}$  evolution in the correlation experiments (Bennett et al., 1995). The TPPM decoupling was optimised directly on the SH3 domain preparations, yielding pulse lengths of typically  $7.0\ \mu\text{s}$  for a phase-modulation angle of 15 degrees. For the specific CP, RF powers corresponding to nutation frequencies of  $\sim 15\ \text{kHz}$  ( $^{15}\text{N}$ ) and  $\sim 20\ \text{kHz}$  ( $^{13}\text{C}$ ) were applied. The amide  $^{15}\text{N}$  were irradiated close to resonance and the  $\text{C}^\alpha$  off-resonance. The  $^{13}\text{C}$  offset was optimised for maximal  $\text{C}^\alpha$  signal, using a 1D version of the pulse program shown in Figure 1B (i.e., without the evolution periods  $t_1$  and  $t_2$ ).

## Results and discussion

An initial step to the assignment of the amide signals can be taken by a combined evaluation of 2D  $^1\text{H}$ - $^{15}\text{N}$  and  $^{15}\text{N}$ - $^{15}\text{N}$  correlation spectra. Figure 2A shows a contour plot of a 2D  $^1\text{H}$ - $^{15}\text{N}$  heteronuclear dipolar correlation spectrum of uniformly  $^{15}\text{N}$  labelled  $\alpha$ -spectrin SH3 domain. The data were obtained at a field of 17.6 T with the sequence depicted in Figure 1A, using  $^1\text{H}$ -homonuclear decoupling during proton evolution. A cross-polarisation contact of  $170\ \mu\text{s}$  was applied to build-up heteronuclear  $^1\text{H}$ - $^{15}\text{N}$  correlations. This short contact time ensures that the spectrum is selective in the sense that only correlations between directly bonded NH pairs are observed. For these strongly coupled spin-pairs, coherent transfer leads to a rapid rise in the  $^{15}\text{N}$  signal intensity during the first  $\sim 150\ \mu\text{s}$  of the CP and results in strong correlations that contain the relevant information. In contrast, the information becomes obscured by proton spin-diffusion processes for longer mixing times ( $>1\ \text{ms}$ ) and the selectivity is lost, although some additional  $^{15}\text{N}$  signal intensity may be obtained. In Figure 2B, a 2D  $^{15}\text{N}$  correlation spectrum is shown, that was recorded at a field of 17.6 T using a standard PDSM mixing unit (Szeverenyi et al., 1982) and is used as a ruler in the assignment procedure. A long PDSM mixing time of 4.0 s was applied to exchange magnetisation between the weakly coupled  $^{15}\text{N}$  spins. Analysis of the  $^{15}\text{N}$ - $^{15}\text{N}$  PDSM experiment revealed that most of the observed cross-peaks are related to transfers between the amide  $^{15}\text{N}$  spins of sequential residues. As an example, the corre-

Table 1. Solid state and solution NMR assignment of the  $^1\text{HN}$  and  $^{15}\text{N}$  signals of the  $\alpha$ -spectrin SH3 domain

Residue	Chemical shift (ppm)					
	Solid <sup>a</sup>		Liquid <sup>a</sup> (pH 7.3)		Liquid <sup>a</sup> (pH 3.5)	
	N	H	N	H	N	H
L8	120.6	8.0	122.8	8.5	123.1	8.48
V9	111.1	8.8	111.2	9.0	111.7	9.17
L10	123.9	9.1	122.7	8.7	123.1	8.97
A11	127.8	9.2	126.7	9.0	127.0	9.12
L12	128.1	9.1 <sup>b</sup>	128.1	9.1	127.5	9.25
Y13	110.1	7.0	111.1	6.9	111.5	7.13
D14	117.6	8.4	117.7	8.2	117.7	8.31
Y15	118.8	8.5	119.3	8.5	120.0	8.74
Q16	127.0	7.6	126.5	7.4	126.8	7.54
E17	122.7	7.7	122.8	7.7	122.9	7.98
K18	119.5	8.6	120.5	8.7	120.6	8.83
S19	111.4	7.1	114.5	7.3	115.0	7.67
P20	137.7	–	133.9	–	133.9	–
R21	112.4 <sup>b</sup>	8.1 <sup>b</sup>	113.3	7.6	113.6	7.69
E22	122.8	7.6	121.9	7.7	121.4	7.87
V23	112.1	7.5	111.7	7.2	113.2	7.39
T24	116.6	6.5	117.1	6.7	118.5	7.23
M25	121.4	9.3	121.8	9.3	121.9	9.53
K26	125.0	9.0	124.9	9.0	124.5	8.97
K27	122.2	9.2	122.3	9.0	122.3	9.05
G28	116.7	8.8 <sup>b</sup>	115.9	8.7	115.6	8.86
D29	122.0	8.4	122.7	8.3	122.1	8.53
I30	120.1	8.7	120.1	7.9	120.2	8.09
L31	128.6	9.5	127.4	9.1	127.2	9.33
T32	119.1	8.2	117.6	8.3	117.1	8.47
L33	130.3	8.9	128.9	8.9	128.9	9.07
L34	125.8	8.9	126.6	8.9	126.0	9.05
N35	114.0	7.4	113.5	7.3	113.8	7.62
S36	125.2	9.2	124.2	9.1	123.7	9.18
T37	112.8	8.1	114.8	8.0	115.0	8.17
N38	126.0	9.1	122.8	8.5	122.3	8.68
K39	121.5	8.6	120.8	8.4	120.8	8.50
D40	115.6	8.0	114.9	8.0	114.4	8.19
W41	123.2	8.4	122.9	8.1	122.5	8.19
W42	124.1	9.0 <sup>b</sup>	124.7	9.2	124.6	9.39
K43	123.6	8.9	124.0	8.7	124.1	8.89
V44	122.2	9.3	122.1	9.2	122.1	9.41
E45	119.5	8.1	119.1	8.4	118.6	8.71
V46	125.7	8.9	124.8	8.7	124.8	8.87
R49	122.1	8.4	120.3	8.0	120.4	8.19
Q50	116.7	8.4 <sup>b</sup>	118.1	8.3	118.6	8.48
G51	107.1	8.7	107.4	8.5	107.2	8.66
F52	118.8	9.0 <sup>b</sup>	118.8	8.9	119.0	9.2
V53	110.3	8.8	110.4	8.8	110.9	9.07
P54	136.8	–	137.4	–	137.4	–
A55	129.1	7.4	129.0	7.3	128.9	7.49
A56	113.2	7.9	113.2	7.8	113.2	7.85
Y57	113.4	7.3	116.5	7.6	115.9	7.72
V58	110.8	7.3	111.1	7.2	110.9	7.43
K59	119.7	8.6	118.4	8.4	118.5	8.65
K60	126.9	9.2	125.8	9.0	125.6	9.2
L61	126.1	8.1	126.4	8.1	125.2	8.45
D62	128.4	7.8	127.3	7.9	123.9	7.98

<sup>a</sup>At T = 298 K.

<sup>b</sup>Resolved from the 3D spectrum (T = 280 K).

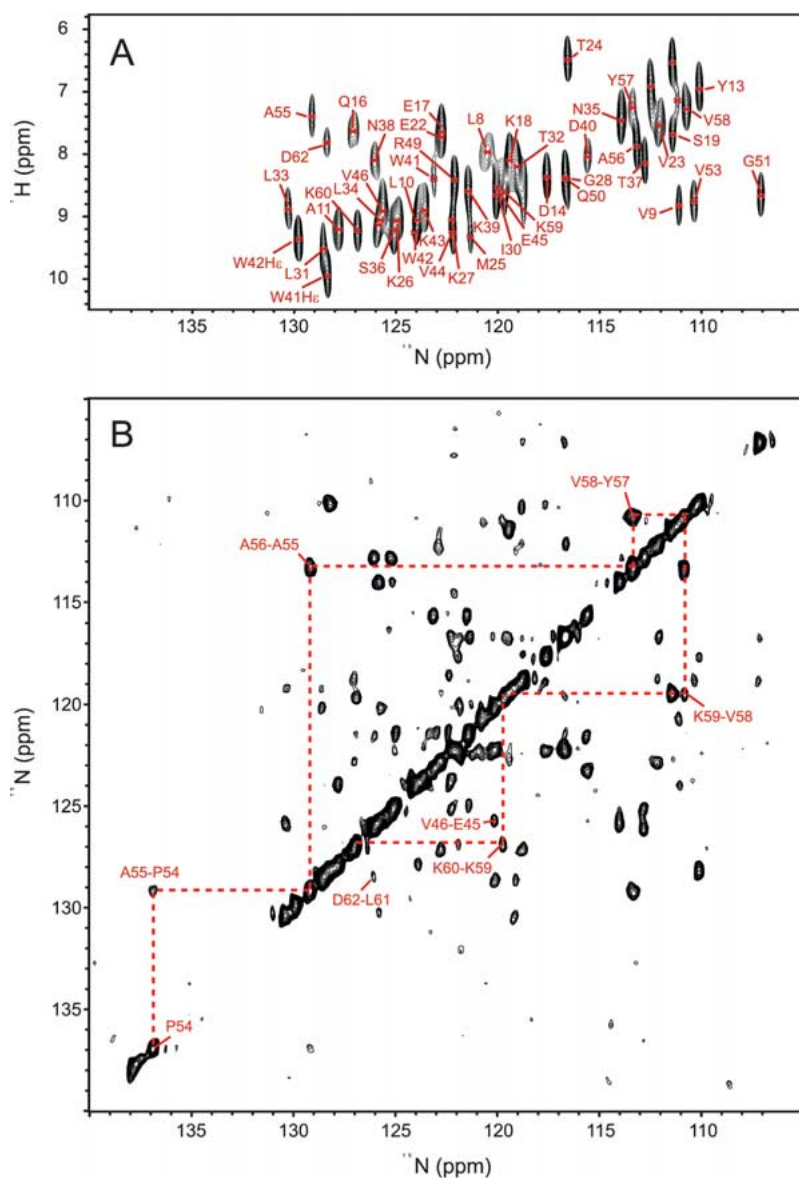


Figure 2. (A) Contour plot of a 2D PMLG-decoupled  $^1\text{H}$ - $^{15}\text{N}$  heteronuclear dipolar correlation spectrum of precipitated ( $U$ - $^{15}\text{N}$ )  $\alpha$ -spectrin SH3 domain, recorded at a field of 17.6 T and with a spinning frequency  $\omega_R/2\pi = 8.0$  kHz. The data were obtained at a temperature of 298 K, using a short ramped CP contact of 170  $\mu\text{s}$ . (B) Contour plot of a 2D  $^{15}\text{N}$ -homonuclear dipolar correlation spectrum of precipitated ( $U$ - $^{15}\text{N}$ )  $\alpha$ -spectrin SH3 domain, recorded at a field of 17.6 T, with a spinning frequency  $\omega_R/2\pi = 8.0$  kHz and at a temperature of 298 K. The data were obtained using a PDSM mixing time of 4.0 s. The dashed line indicates the correlation walk from P54 to K60. Note that the amides of A56 and Y57 have almost identical chemical shifts and a cross-peak can not be resolved from the diagonal.

lations in the subsequence P54 to K60 are depicted in Figure 2B. Other cross-peaks could be identified and assigned in a similar fashion and the chemical shifts are listed in Table 1.

Due to the selectivity and the high resolution in the  $^{15}\text{N}$  dimension, a large number of NH signals can be assigned unambiguously from the 2D exper-

iment of Figure 2A (Table 1). There is, however, for a small number of NH pairs overlap of the  $^{15}\text{N}$  chemical shifts, which prohibits the complete proton assignment on the basis of the 2D  $^1\text{H}$ - $^{15}\text{N}$  dataset only. Additional resolution enhancement can be achieved by exploiting the relatively well-resolved correlations in a NCA experiment (Pauli et al., 2001). This can be

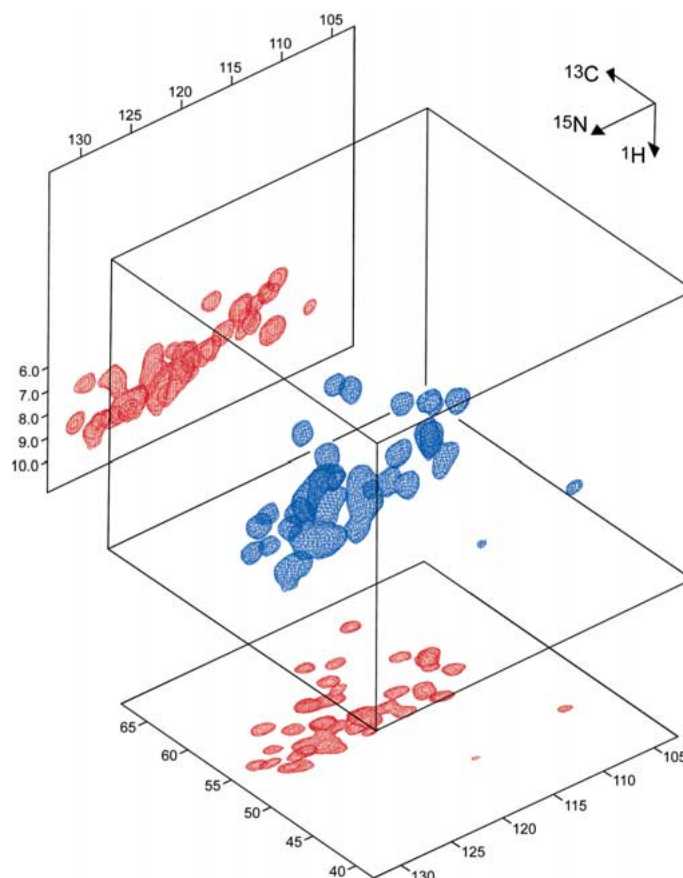


Figure 3. Plot of a 3D PMLG-specific CP HNCA correlation experiment, displayed with a single contour (blue). The 3D dataset was recorded from precipitated ( $U$ - $^{15}\text{N}$ ,  $^{13}\text{C}$ )  $\alpha$ -spectrin SH3 domain, at a field of 9.4 T and at a spinning frequency  $\omega_R/2\pi = 8.0$  kHz. The spectrum was obtained at a temperature of 280 K. The  $\omega_1$ - $\omega_2$  ( $^1\text{H}$ - $^{15}\text{N}$ ) and  $\omega_2$ - $\omega_3$  ( $^{15}\text{N}$ - $^{13}\text{C}$ ) projections of the 3D experiment are shown in red.

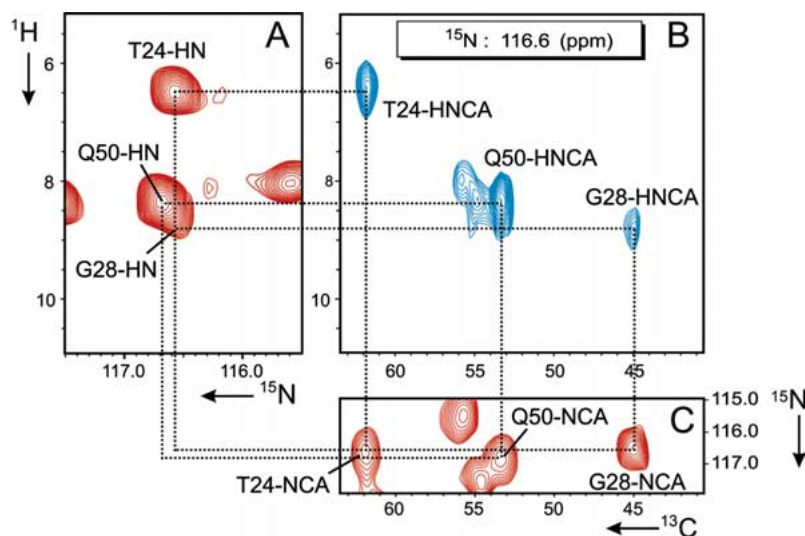


Figure 4. Assignment of the amides of T24, G28 and Q50. (A) shows a section of the 2D  $^1\text{H}$ - $^{15}\text{N}$  experiment of Figure 2A, centred around the  $^{15}\text{N}$  chemical shift of the three residues ( $\sim 116.6$  ppm). In (B), a plane from the 3D dataset is shown, extracted at the same  $^{15}\text{N}$  chemical shift. Finally, (C) shows a strip from a 2D NCA experiment, recorded from ( $U$ - $^{15}\text{N}$ ,  $^{13}\text{C}$ )  $\alpha$ -spectrin SH3 domains at a field of 9.4 T and using a spinning frequency  $\omega_R/2\pi = 8.0$  kHz.

done by correlating the  $^1\text{H}$ - $^{15}\text{N}$  signal with the  $\text{C}^\alpha$  of the same residue in a 3D ( $^1\text{H}$ - $^{15}\text{N}$ - $^{13}\text{C}$ ) heteronuclear correlation experiment (Figure 3), using the pulse sequence shown in Figure 1B. The method combines the PMLG-decoupled  $^1\text{H}$ - $^{15}\text{N}$  experiment in Figure 1A with specific CP following the nitrogen evolution in  $t_2$  (Baldus et al., 1998), to transfer magnetisation selectively from the backbone  $^{15}\text{N}$  to the  $\text{C}^\alpha$ . In this way, each residue gives rise to a single intra-residue  $^1\text{H}^{\text{N}}$ - $^{15}\text{N}$ - $^{13}\text{C}^\alpha$  correlation in the 3D spectrum. The resolution enhancement obtained in the 3D HNCA correlation experiment allows unambiguous assignments of the amide protons. This is illustrated in Figure 4 for the residues T24, G28 and Q50. Figure 4A shows a section of the 2D  $^1\text{H}$ - $^{15}\text{N}$  dataset in Figure 2A, with the  $^{15}\text{N}$  centred around 116.5 ppm, close to the amide  $^{15}\text{N}$  chemical shift for the three residues. Due to overlap in the nitrogen dimension, it is not possible to assign the amide protons of T24, G28 and Q50 unambiguously from the 2D experiment. On the other hand, the  $\text{C}^\alpha$  resonate with different chemical shifts for T24, Q50 and G28, at 61.9 ppm, 53.4 ppm and 45.1 ppm, respectively. Hence the signals from the three residues are fully resolved in the NCA dimension of the experiment (cf. Figures 4B and C) and the three amide protons can be assigned unambiguously from the  $\omega_1$ - $\omega_3$  slice extracted from the 3D dataset with an  $\omega_2$   $^{15}\text{N}$  shift near 116.6 ppm (Figure 4B). The assignment of the amide protons is listed in Table 1, together with the shifts found in solution NMR, for pH 3.5 and pH 7.5. The  $^1\text{H}^{\text{N}}$  that we could not detect are from the first seven residues on the N-terminus (M1-E7), and from the residues N47 and D48.

The  $^{15}\text{N}$ - $^{15}\text{N}$  correlation network along the protein backbone observed in the  $^{15}\text{N}$ - $^{15}\text{N}$  correlation spectrum was useful for cross-checking our previously reported  $^{15}\text{N}$  assignment (Pauli et al., 2001). Two more  $^{15}\text{N}$  signals were identified that were not previously assigned from the NCA-type experiments (Pauli et al., 2001). D62 at the C-terminus was tentatively assigned by cross-peaks involving L61, and the backbone amide signal of V46 was identified from correlations with E45 (Figure 2B). Consistently, a weak correlation was observed in a 2D NCA spectrum of a ( $^{13}\text{C}$ ,  $^{15}\text{N}$ ) SH3 sample recorded at 9.4 T, that we now can assign to V46 (data not shown). This correlation has a chemical shift of 125.7 ppm for the  $^{15}\text{N}$  and of 60.0 ppm for the  $^{13}\text{C}^\alpha$ , in line with the previously reported  $\text{C}^\alpha$  assignment (Pauli et al., 2001). Combining these assignments with the 2D  $^1\text{H}$ - $^{15}\text{N}$  and 3D  $^1\text{H}$ - $^{15}\text{N}$ - $^{13}\text{C}$  experiments, the

amide proton signals of V46 and D62 can be assigned and are included in Table 1.

Residues that are difficult to assign from the  $^{15}\text{N}$ - $^{15}\text{N}$  PDSM experiment are prolines because most of the correlations involving the back-bone nitrogens of these residues are very weak and below the limit set by the contours in Figure 2B. Proline is the only type of residue that has a non-protonated amide nitrogen, and coherence transfer mediated by  $^{15}\text{N}$  signal broadening induced by NH dipolar couplings during the PDSM mixing will be less effective. Since prolines resonate downfield of the amide response, the PDSM sequence can be expected to be less efficient for  $^{15}\text{N}$  magnetisation transfer between prolines and residues that resonate more upfield. Indeed, transfer between the amides of P54 and A55 is observed, that have relatively closely spaced chemical shifts of 136.8 ppm and 129.2 ppm, respectively, but not between P54 and V53, the latter resonating around 110 ppm. Likewise, sequential correlations between P20 (137.7 ppm) and S19 (111.4 ppm) or R21 (112.3 ppm), that have a large difference in chemical shift, are not detected.

Some correlations were detected in the 2D  $^{15}\text{N}$ - $^{15}\text{N}$  spectrum that could not be assigned to transfers between amides of sequential residues. Such correlations involve long-range transfers and provide restraints for the calculation of the fold of the SH3 domain from the solid-state NMR data (Castellani et al., 2002). For instance, a correlation is observed that can be identified as V23-F52 and/or V23-Y15. According to the solution NMR structure of the  $\alpha$ -spectrin SH3 domain (Blanco et al., 1997), the distance between the amides is 4.1 Å for V23 and F52, and 9.0 Å for V23 and Y15. The observed correlation most likely involves transfer over the shortest distance, between V23 and F52. Likewise, it was found that S19 correlates with E17 (5.8 Å) and/or E22 (4.9 Å). Since the long-range correlations can not be assigned unambiguously from the current solid-state data, they were included as ‘ambiguous’ restraints in the structure calculations presented recently (Castellani et al., 2002).

## Conclusion

It has been shown that amide proton signals can be assigned unambiguously from the 2D and 3D dataset in Figures 2–4, providing that  $^{13}\text{C}$  and  $^{15}\text{N}$  assignments exist. Together with the assignment of the non-exchanging protons reported previously (van Rossum

et al., 2001), nearly all  $^1\text{H}$  of the  $\alpha$ -spectrin SH3 domain have been assigned. This is the largest system for which a nearly full  $^1\text{H}$  solid-state MAS NMR assignment has been obtained till date. Most of the cross-peaks in the triple-resonance experiment are fully resolved, even at a moderately low field strength of 9.4 T. The 3D spectrum may also serve as a potentially important building block for obtaining structural restraints, if combined with suitable homonuclear or heteronuclear transfer schemes. In addition, the 3D HNCA experiment is considerably more resolved as compared to the 2D NCA experiment recorded at the same magnetic field strength (Pauli et al., 2001). The resolution enhancement achieved by adding the  $^1\text{H}$  dimension to the NCA experiment may be instrumental for the sequential assignment, if combined with HNCO experiments performed in parallel.

The  $^{15}\text{N}$  assignment obtained from the  $^{15}\text{N}$ - $^{15}\text{N}$  correlation experiment is fully consistent with the assignment reported previously (Pauli et al., 2001). In this respect, the  $^{15}\text{N}$  chemical shift information contained in the  $^{15}\text{N}$  homonuclear correlation experiment is basically the same as the one obtained from the NCA/NCO-type triple resonance experiments. The experiment 'tells' which pairs of  $^{15}\text{N}$  correlate and provides information about which amides are connected via sequential residues. Hence, the  $^{15}\text{N}$ - $^{15}\text{N}$  experiment provides an independent check of the  $^{15}\text{N}$  assignments, since it relies on direct transfer between the sequential  $^{15}\text{N}$  of the protein backbone and not on a two-step transfer mechanism via the  $\text{C}^\alpha$  and/or CO. It should therefore be considered as an experiment that can be performed in parallel with the NCA(CX) and NCO(CX) experiments (Pauli et al., 2001), to facilitate the assignment, and to reduce ambiguity in an early stage in the assignment procedure.

### Acknowledgements

Support from the DFG (grant no.: SFB 449) and from the EU (grant no.: BIO4-CT97-2101) is gratefully acknowledged. The authors thank Bernd Reif for helpful discussion.

### References

- Baldus, M., Petkova, A.T., Herzfeld, J. and Griffin, R.G. (1998) *Mol. Phys.*, **95**, 1197–1207.
- Bennett, A.E., Rienstra, C.M., Auger, M., Lakshmi, K.V. and Griffin, R.G. (1995) *J. Chem. Phys.*, **103**, 6951–6958.
- Blanco, F.J., Ortiz, A.R. and Serrano, L. (1997) *J. Biomol. NMR*, **9**, 347–357.
- Brown, S.P., Zhu, X.X., Saalwachter, K. and Spiess, H.W. (2001) *J. Am. Chem. Soc.*, **123**, 4275–4285.
- Castellani, F., van Rossum, B., Diehl, A., Schubert, M., Rehbein, K. and Oschkinat, H. (2002) *Nature*, **420**, 98–102.
- Griffin, R.G. (1998) *Nat. Struct. Biol. NMR Suppl.*, **7**, 508–512.
- Hohwy, M., Jaroniec, C.P., Reif, B., Rienstra, C.M. and Griffin, R.G. (2000) *J. Am. Chem. Soc.*, **122**, 3218–3219.
- Hong, M. (1999) *J. Biomol. NMR*, **15**, 1–14.
- Hong, M., Gross, J.D. and Griffin, R.G. (1997) *J. Phys. Chem.*, **B101**, 5869–5874.
- McDermott, A., Polenova, T., Bockmann, A., Zilm, K.W., Paulson, E.K., Martin, R.W., Montelione, G.T. and Paulsen, E.K. (2000) *J. Biomol. NMR*, **16**, 209–219.
- Pauli, J., Baldus, M., van Rossum, B., de Groot, H. and Oschkinat, H. (2001) *Chembiochem*, **2**, 272–281.
- Pauli, J., van Rossum, B., Forster, H., de Groot, H.J.M. and Oschkinat, H. (2000) *J. Magn. Reson.*, **143**, 411–416.
- Reif, B., Hohwy, M., Jaroniec, C.P., Rienstra, C.M. and Griffin, R.G. (2000) *J. Magn. Reson.*, **145**, 132–141.
- Schnell, I., Brown, S.P., Low, H.Y., Ishida, H. and Spiess, H.W. (1998) *J. Am. Chem. Soc.*, **120**, 11784–11795.
- Song, X. and McDermott, A.E. (2001) *Magn. Reson. Chem.*, **39**, 37–43.
- Straus, S.K., Bremi, T. and Ernst, R.R. (1998) *J. Biomol. NMR*, **12**, 39–50.
- Szeverenyi, N.M., Sullivan, M.J. and Maciel, G.E. (1982) *J. Magn. Reson.*, **47**, 462–475.
- van Rossum, B.J., Castellani, F., Rehbein, K., Pauli, J. and Oschkinat, H. (2001) *Chembiochem*, **2**, 906–914.
- Vinogradov, E., Madhu, P.K. and Vega, S. (1999) *Chem. Phys. Lett.*, **314**, 443.
- Wu, C.H., Ramamoorthy, A. and Opella, S.J. (1994) *J. Magn. Reson.*, **A109**, 270–272.
- Zhao, X., Sudmeier, J.L., Bachovchin, W.W. and Levitt, M.H. (2001) *J. Am. Chem. Soc.*, **123**, 11097–11098.